Critical phenomena at the spin-Peierls transition in MEM(TCNQ)$_2$

M. D. Lumsden and B. D. Gaulin
Department of Physics and Astronomy, McMaster University, Hamilton, Ontario, Canada L8S 4M1
(Received 21 September 1998)

We have performed a detailed x-ray scattering study of the critical phenomena associated with the spin-Peierls phase transition in the organic compound MEM(TCNQ)$_2$. Analysis of the superlattice reflection intensity indicates an order parameter with an associated critical exponent $\beta = 0.35 \pm 0.06$ consistent with three-dimensional behavior, as seen in the inorganic compound $CuGeO_3$, and clearly inconsistent with mean field behavior, as indicated in previous studies. Measurements of lattice constants indicate the presence of spontaneous strains below the transition temperature. The measured critical scattering is not well described by an Ornstein-Zernike, Lorentzian line shape. An adequate description is obtained with a Lorentzian^x with x varying or with a Lorentzian+Lorentzian^2 line shape. The latter descriptor is reminiscent of previous high-resolution x-ray scattering studies where a two-component line shape has been observed. Analysis using such a line shape indicates critical exponents γ and ν, obtained from the Lorentzian component, consistent with the results obtained for the order parameter. [S0163-1829(99)05813-0]

I. INTRODUCTION

The spin-Peierls (SP) transition[1] occurs in antiferromagnetic Heisenberg spin-1/2 chains in the presence of strong magnetoelastic coupling with three-dimensional (3D) lattice vibrations. Below the SP transition temperature (T_{sp}), a lattice dimerization occurs which increases progressively as the temperature is lowered, together with the concomitant appearance of an energy gap in the spectrum of magnetic excitations. This gap separates a nonmagnetic singlet ground state from a triplet of excited states. Such a transition is characterized by a rapid, isotropic drop in the magnetic susceptibility below T_{sp}, due to the nonmagnetic nature of the ground state, the appearance of a gap in the excitation spectrum, and the appearance of new, superlattice Bragg peaks resulting from new periodicities introduced by the lattice dimerization.

The organic compound MEM(TCNQ)$_2$ is composed of planar TCNQ molecules which stack along the crystallographic $(0,0,l)$ direction producing quasi-one-dimensional chains.[2] Above 335 K, the chains are uniform and the system is metallic, but at this temperature, MEM(TCNQ)$_2$ undergoes a metal-insulator transition, characterized as an electronic Peierls transition,[3] and the uniform chains become dimerized. Between 335 K and 17.1 K, there is a single spin-1/2 magnetic moment present on each dimer and the crystal structure is triclinic with lattice parameters $a = 7.824(5)$ Å, $b = 15.426(16)$ Å, $c = 6.896(5)$ Å, $\alpha = 113.59(8)°$, $\beta = 73.27(7)°$, and $\gamma = 112.71(8)°$ at 113 K.[4] At 17.1 K, MEM(TCNQ)$_2$ undergoes an additional phase transition producing a second dimerization of the chains.[4] This second transition has been shown to exhibit all of the characteristics of a SP phase transition. The uniform drop in the magnetic susceptibility[2,5] and the appearance of superlattice Bragg peaks with indices $(h,k,l/2)$[4,6] have been observed (these Miller indices and those quoted in the remainder of this paper refer to the room temperature crystal structure, not the structure above the 335 K transition). The gap in the excitation spectrum has not been directly observed with inelastic neutron scattering due to the low density of magnetic moment,[7] but its presence has been inferred from recent muon spin resonance studies.[8] Finally, the characteristic behavior in a magnetic field has been observed,[9] where T_{sp} decreases with increasing field until a critical field is reached, above which the system enters into a different, incommensurate phase.[1]

The critical phenomena associated with the SP transition have not been well characterized. The most comprehensive work has involved measurements of the exponent β associated with the order parameter in the inorganic SP compound $CuGeO_3$ where an exponent $\beta = 0.345 \pm 0.03$ was found consistent with a 3D universality class.[10] Measurements of the exponents γ and ν associated with the buildup of fluctuations upon nearing the transition temperature have been very difficult to obtain in $CuGeO_3$. The majority of scattering studies has had great difficulty in observing any critical scattering[10–13] with the only success occurring using synchrotron x-ray radiation.[14] However, in these synchrotron studies, the observed critical scattering could not be described using a standard Ornstein-Zernike form, which yields a Lorentzian line shape in the wave vector, but instead a much sharper line shape, well described by a Lorentzian squared, was observed. As is typically the case with this so-called ''second length scale'' critical scattering,[15] the extracted critical exponents are larger in magnitude than expected and are inconsistent with any conventional universality class.

Examination of critical properties in organic SP systems has been less comprehensive with the only existing results indicating behavior consistent with mean field theory.[3,16] This motivated us to carefully measure both the order parameter and the critical fluctuations associated with the SP transition in the organic compound MEM(TCNQ)$_2$. Previous studies indicated the presence of substantial critical scattering but no quantitative line shape analysis had been performed.[4] We expected that the presence of second length scattering which complicated the critical fluctuation measurements in $CuGeO_3$ (Ref. 14) would not occur in MEM(TCNQ)$_2$. These sharp fluctuations are generally at-

tributed to defects in the near-surface region[15] and are much more prevalent in x-ray scattering measurements where low penetration depths result in substantial surface sensitivity. However, the organic nature of $MEM(TCNQ)_2$ yields large x-ray penetration depths and consequently reduced surface sensitivity. Thus, we anticipated a single Lorentzian line shape would be adequate to describe the critical scattering, as is typically seen in bulk neutron scattering measurements, allowing critical exponents consistent with traditional universality classes to be extracted.

In addition, we performed measurements of the thermal expansion of $MEM(TCNQ)_2$ in the vicinity of the SP transition temperature. Similar measurements on $CuGeO_3$ (Refs. 13, 17, and 18) indicated the presence of spontaneous strains below the transition temperature which scaled with the square of the order parameter.

II. EXPERIMENTAL DETAILS

A single crystal of $MEM(TCNQ)_2$ with approximate dimensions $4\times1\times0.5$ mm^3 was mounted in a Be can in the presence of a He exchange gas. This sample was part of the larger crystal used in Ref. 4. This can was mounted on the cold finger of a closed-cycle He refrigerator and the temperature was kept stable to ±0.01 K for all reported measurements. The measurements were performed in a Huber four-circle diffractometer, allowing access to a large portion of reciprocal space, and the incident radiation was Cu Kα radiation from a Rigaku 18 kW rotating anode x-ray generator. This radiation was further monochromatized by a flat PG (0,0,2) monochromator crystal.

The order parameter was measured at several wave vectors to ensure reproducible results. The critical scattering was measured at both the $(1,6,-1/2)$ and (0,11,3/2) superlattice peaks as a check for consistency, these peaks being chosen due to their relative intensity when compared with approximately 120 other superlattice peaks. For the measurements of the thermal expansion, the (0,12,0) and (0,0,4) Bragg peaks were examined and the resolution was improved significantly by tightening the collimation which is controlled by a series of four slits, two before and two after the sample position.

III. ORDER PARAMETER

A. Experiment

The temperature dependence of the peak intensity of the $(1,6,-1/2)$, (0,11,3/2), (1,5,3/2), and (0,0,5/2) superlattice reflections was measured for temperatures ranging from 10 K to 20 K and the resulting peak intensity as a function of temperature for the (0,11,3/2) reflection is shown in the upper panel of Fig. 1. In addition, the temperature dependence of the intensity integrated over a transverse scan was measured from 15 K to 18 K for the $(1,6,-1/2)$ reflection. The results for all four peaks are consistent with one another, leading to the conclusion that extinction effects are small as the peak intensities of the various reflections differed greatly [for instance, the (0,0,5/2) reflection produced a rather low peak intensity of about 150 counts/sec while the (0,11,3/2) reflection was much more intense yielding a count rate of about 4200 counts/sec].

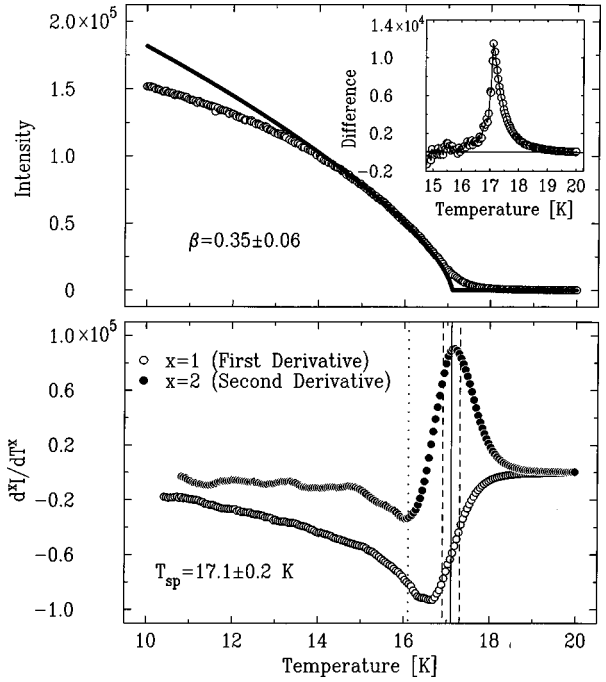

FIG. 1. The upper panel shows the peak intensity as a function of temperature for the (0,11,3/2) superlattice reflection. The solid line represents the best fit to a simple power law, Eq. (1), with a value of the exponent β of about 0.35 and the inset shows the difference between this line and the measured intensity. Such a difference indicates the contribution due to fluctuations. The lower panel shows the first and second derivatives of the peak intensity as a function of temperature. The dotted line indicates the temperature above which fluctuations become substantial. The solid line and nearby dashed lines represent the best fit and extreme estimates of the transition temperature, respectively.

B. Analysis

Determination of the transition temperature was achieved by careful examination of the peak intensity as a function of temperature and its first and second derivatives as shown in the lower panel of Fig. 1. In the absence of any critical scattering, one expects the first derivative to jump abruptly to zero at the transition temperature. However, critical scattering from fluctuations provides an additional contribution to the peak intensity which reaches its maximum value in **Q** at the ordering wave vector and in temperature at the transition temperature. Consequently, this critical scattering generates substantial curvature in the peak intensity near T_{sp}, causing the first derivative to change in a much more gradual fashion. The range of temperatures over which this critical scattering is substantial relative to the Bragg component must be eliminated from the analysis to obtain accurate estimates of the critical exponent β. The observed first derivative can be seen to decrease steadily until about 16.3 K where it appears to level out. We take this to indicate the presence of substantial critical scattering and, consequently, the analysis was performed up to a maximum temperature of about 16.1 K, chosen as a conservative estimate, in order to consider data containing solely the Bragg component. This upper temperature is represented by the dotted, vertical line in the lower panel of Fig. 1.

The second derivative of the peak intensity as a function of temperature is also shown in the lower panel of Fig. 1. It

can be seen to be strongly peaked at a temperature of about 17.1 K and this point, representing the point of maximum curvature, is taken to be indicative of the transition temperature. This maximum point could only be determined accurately to approximately ± 0.2 K and thus we determine the transition temperature to be 17.1 ± 0.2 K. This best estimate and the maximum and minimum values are represented by the solid line and two dashed lines, respectively, in the lower panel of Fig. 1.

To avoid difficulties resulting from changes in peak position, measurements of the intensity integrated over a transverse scan were performed on the $(1,6,-1/2)$ superlattice reflection from 15 K up to about 18 K and these data will be used in the quantitative analysis which follows. In order to extract the proper critical behavior of the order parameter, these data were fit to a power law in the reduced temperature, $t = 1 - T/T_{sp}$,

$$\text{intensity} = I_0 t^{2\beta} + \text{background}. \tag{1}$$

This power law behavior is expected to be valid in the asymptotic critical region, near T_{sp}, where the length scale associated with the fluctuations in the order parameter dominates over any other relevant length scales in the system. As the temperature is lowered below this region, this power law behavior must be modified by successive correction-to-scaling terms,[19] the first of which is included in Eq. (2),

$$\text{intensity} = I_0 t^{2\beta}(1 + At^{\Delta}) + \text{background}, \tag{2}$$

where the exponent Δ has an approximate value of 0.5 for 3D behavior.

To investigate the extent of the asymptotic region, the dependence of the extracted value of β on the lowest temperature included in the fits was examined carefully and is shown in Fig. 2 for fits to the ordinary power law, Eq. (1), from 15 K up to the predetermined maximum temperature of 16.1 K. The plot presents results with the transition temperature fixed at the nominal value of 17.1 K and the maximum and minimum temperatures of 17.3 K and 16.9 K, respectively. Fits were also performed using the ordinary power law with a varying transition temperature. In all cases, the best fit value of T_{sp} fell within the previously determined range of values, namely, between 16.9 K and 17.3 K, validating the previously selected transition temperature. The results obtained with a fixed T_{sp} of 17.1 K indicate no systematic behavior with respect to the lowest temperature included in the fits, producing a value of β of about 0.35. The upper and lower bounds to T_{sp} generate values of the exponent β approximately ± 0.06 around this nominal value. This error, determined by the error in the transition temperature, is by far the largest source of uncertainty in determination of the critical exponent and thus we arrive at an exponent $\beta = 0.35 \pm 0.06$. This value of β is consistent with conventional 3D behavior, as was observed in $CuGeO_3$,[10] and is clearly inconsistent with mean field behavior, as reported in previous studies.[3] For reference, the values of the exponent β for 3D Ising, XY, and Heisenberg universality[20] are indicated in Fig. 2.

The robust behavior of the fits using the ordinary power law with respect to the range of data included suggests that the asymptotic region extends to at least 15 K. To check that this is indeed the case, the same examination of β as a function of lowest temperature was performed using the power law with first correction to scaling included, Eq. (2). The resulting extracted values of β agreed precisely with those resulting from the ordinary power law, Eq. (1), confirming that correction terms are unnecessary for temperatures as low as 15 K.

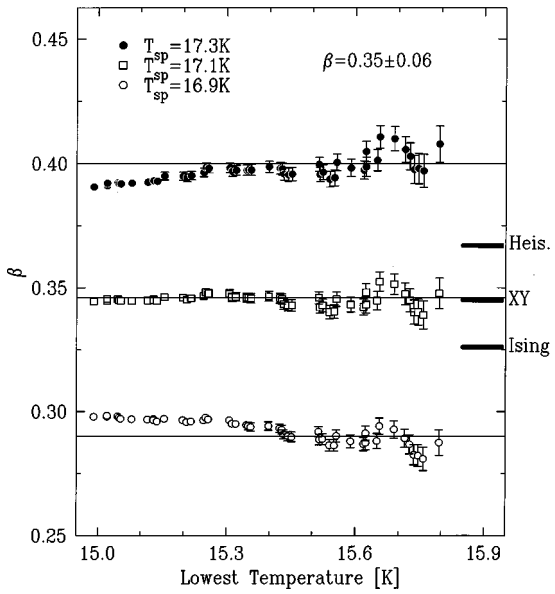

FIG. 2. The extracted value of the exponent β obtained from the ordinary power law, Eq. (1), as a function of the lowest temperature included in the fits with T_{sp} fixed at values of 17.1 K, 17.3 K, and 16.9 K representing the best estimate, maximum, and minimum values, respectively. The robust nature of the fits with respect to the lowest temperature is indicative of an asymptotic region which extends at least until 15 K. For reference, the theoretical predictions for 3D Ising, XY, and Heisenberg universality are indicated on the plot.

The solid line shown in the upper panel of Fig. 1 represents the best fit to Eq. (1) with a corresponding exponent β of 0.35. The difference between the data and this solid line is shown, for temperatures near the transition temperature, in the inset to the upper panel of Fig. 1. This difference, representing the contribution to the peak intensity resulting from the critical fluctuations, can be seen to peak sharply at the transition temperature. One expects the same critical behavior above and below the transition temperature, but the amplitude of the power law describing the fluctuations should be smaller below T_{sp} due to the universal nature of the amplitude ratio. Consequently, the critical scattering should fall away faster below the transition temperature, a point which is qualitatively clear from the difference data presented in the inset.

C. Comparison to $CuGeO_3$

As mentioned previously, the asymptotic region in $MEM(TCNQ)_2$ extends to at least 15 K corresponding to a value of T/T_{sp} of about 0.88. This is in contrast to the results obtained on $CuGeO_3$ where the first correction to scaling term was needed for temperatures within 0.4 K of the transition temperature, indicating an asymptotic region which extends no further than $T/T_{sp} = 0.96$.

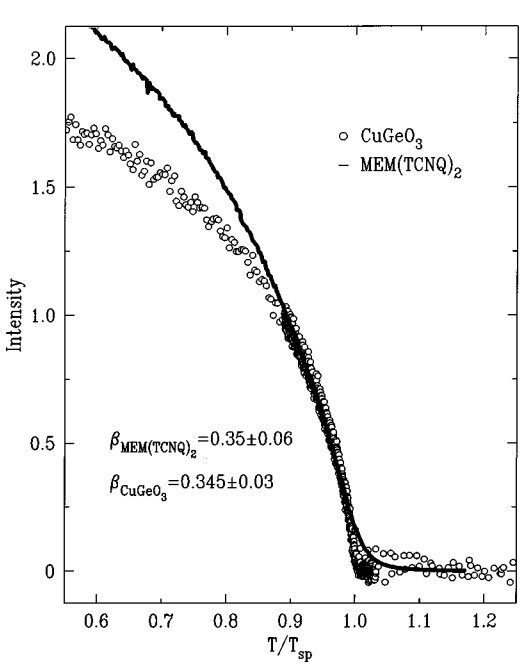

FIG. 3. The peak intensity as a function of temperature normalized to the transition temperature for the inorganic SP compound $CuGeO_3$ and the organic system $MEM(TCNQ)_2$. The intensity is normalized to unity at a T/T_{sp} of about 0.9. There is good agreement between the two close to the transition as indicated by the similar values of the exponent β. The low-temperature noncritical behavior is rather different, suggesting greater ease of deformation for $MEM(TCNQ)_2$.

To allow for a more systematic comparison between $MEM(TCNQ)_2$ and $CuGeO_3$, Fig. 3 shows the peak intensity for both plotted as a function of T/T_{sp} normalized to unity at $T/T_{sp}=0.9$ (this value is chosen as it includes the range in both compounds where the order parameter has been quantitatively examined in detail). We can see agreement between the two from 0.9 to about 0.96, suggesting similar critical behavior as quantitatively shown by the similar values for the exponent β. Above T/T_{sp} of about 0.96, the critical scattering present in $MEM(TCNQ)_2$ and much less evident in $CuGeO_3$ causes the peak intensities to deviate. Below T/T_{sp} of about 0.9, the peak intensity of $CuGeO_3$ seems to saturate much more rapidly with decreasing temperature than does the $MEM(TCNQ)_2$ intensity, indicating very different noncritical behavior between the two compounds. This implies that the $MEM(TCNQ)_2$ lattice is able to deform with greater ease than that of $CuGeO_3$, a fact that may be related to a soft phonon mode present in $MEM(TCNQ)_2$ (Ref. 21) which appears to be absent in $CuGeO_3$. Such deviations may also be related to differences in the nature of the dimerization wave vector which produces a single dimerization along the c^* axis for $MEM(TCNQ)_2$ and a doubly dimerized state, with dimerizations along a^* and c^*, for $CuGeO_3$.

IV. LATTICE CONSTANTS

Measurements of the temperature dependence of the lattice constants in the inorganic SP compound $CuGeO_3$ indicated the presence of spontaneous strains below the transition temperature whose magnitude scaled with the square of the order parameter.[10,13,17,18] We performed similar measurements on the (0,0,4) and (0,12,0) reflections of $MEM(TCNQ)_2$ in search of analogous effects in an organic SP system.

The (0,12,0) reflection was measured using a conventional approach wherein, following a change in temperature, all the angles were rocked and centered and a detailed longitudinal scan performed. The peak position was then extracted from line shape analysis on this longitudinal scan. Such a conventional approach could not produce sufficient sensitivity for the (0,0,4) reflection largely due to inferior resolution at this reflection [the scattering angle for (0,12,0) was $2\theta=86.98°$ while that for (0,0,4) was $2\theta=59.70°$]. To obtain reasonable results for this peak, an alternative approach, described in detail in Ref. 10, was employed. The new approach involves measuring changes in intensity for some point on the sharply varying portion of the line shape and from this, coupled with a detailed knowledge of the line shape itself, the peak position and thus lattice constant as a function of temperature can be extracted. This method assumes a robust line shape over the temperature range of interest, an assumption which is reasonable over a small range of temperatures. The enhancement in sensitivity is accomplished through an improvement in statistics as the time in measuring a single temperature now only includes measuring the intensity at a single point. This results in a measurement which is less intensity limited compared to the conventional approach and allows for improvement in the collimation and, thus, resolution.

The resultant lattice constants as a function of temperature are shown in Fig. 4. The data are plotted as $\Delta d/d$ normalized to zero at a temperature of 25 K. The lower panel shows the results for the (0,12,0) reflection which indicates a clear change in thermal expansion at T_{sp}, indicated by the dashed line, demonstrating the presence of a spontaneous strain, as was observed in $CuGeO_3$. The upper panel shows the results for the (0,0,4) reflection and, while not as evident, appears to similarly show the existence of such a spontaneous strain.

To further emphasize this point, the derivative of the data is shown in the inset for both reflections. Here, one can clearly see an abrupt change in slope at the transition temperature in both reflections, implying the presence of spontaneous strains in both directions. The presence of such strains in $MEM(TCNQ)_2$, coupled with previous observations of similar results in $CuGeO_3$ and in the recently proposed SP system α'-NaV_2O_5,[22] suggests that these spontaneous strains are indeed an inherent characteristic of a SP system.

We attempted to extract the spontaneous strains from the measurements of $\Delta d/d$ to examine whether scaling with the square of the order parameter occurs, as was the case with $CuGeO_3$. However, without some independent measure of the background to be subtracted, representing the thermal expansion in the absence of the SP transition, it is very difficult to properly extract this information. Such an independent background determination was performed in $CuGeO_3$ (Ref. 10) by repeating the measurements on a dilute sample with sufficient dopant concentrations to suppress the SP transition below the temperature range of interest. Low-solubility limits for dopants in $MEM(TCNQ)_2$ make a simi-

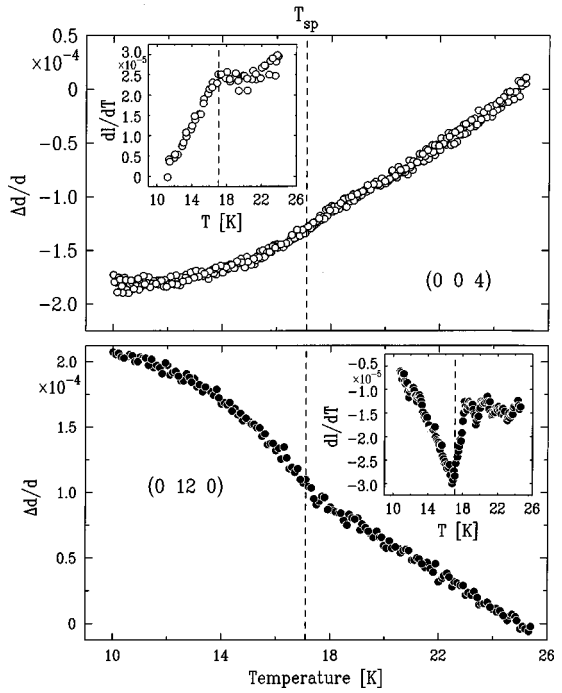

FIG. 4. The relative change in d spacing for the (0,0,4) and (0,12,0) Bragg peaks as a function of temperature. There are clear deviations in the data at the transition temperature, suggesting the presence of spontaneous strains below T_{sp}. To further emphasize this point, the inset in both the upper and lower panels shows the temperature derivative of $\Delta d/d$. This shows a clear change in slope at the transition temperature, emphasizing the presence of spontaneous strains. The value of the transition temperature, $T_{sp} = 17.1$ K, is indicated by the dashed line.

lar study impossible, but perhaps, in the future, these measurements could be repeated in a magnetic field where the transition temperature can be sufficiently suppressed to allow for an independent background determination.

V. CRITICAL SCATTERING

The critical fluctuations accompanying the SP transition were carefully measured at two superlattice wave vectors, $(1,6,-1/2)$ and $(0,11,3/2)$, by performing detailed scans along the principal reciprocal lattice directions at a number of temperatures between 16 K and 20 K. In order to perform quantitative line shape analysis, the anticipated cross section $d\sigma/d\Omega(\mathbf{Q}-\mathbf{Q}')$ must be convoluted with the instrumental resolution function $R(\mathbf{Q}')$,

$$I(\mathbf{Q}) = \int R(\mathbf{Q}') \frac{d\sigma}{d\Omega}(\mathbf{Q}-\mathbf{Q}')\, d\mathbf{Q}'. \tag{3}$$

Determination of the instrumental resolution function was performed by careful measurements at low temperatures (~ 9 K) where the scattering is assumed to be free of any critical scattering, and only a resolution limited Bragg peak remains. It became evident that finding an analytical description to adequately describe this resolution function would be a formidable task due to the existence of two large crystallites of roughly equal size constituting the mosaic single crystal. Figure 5 shows a mesh scan in the h-k reciprocal space plane at a value of l just off the optimized peak position. This contour plot clearly shows the presence of two distinct crystallites.

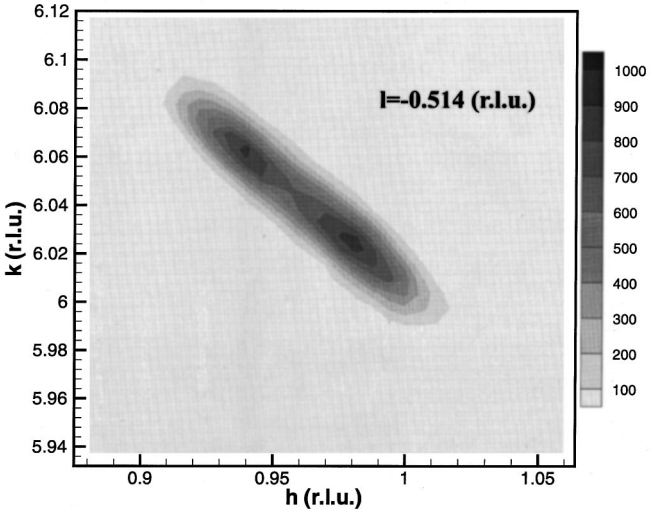

FIG. 5. Low-temperature (~ 9 K) mesh scan through the $(1,6,-1/2)$ superlattice reflection in the h-k reciprocal lattice plane at a value of l slightly off the optimized peak position. This clearly shows the presence of two crystallites in the mosaic single crystal.

Approximately 30 mesh scans, similar to the one shown in Fig. 5, were measured to fully characterize the resolution function at all points in h, k, l space in the vicinity of the superlattice reflection. The two measured reflections were chosen due to their relative strength when compared to other reflections and to allow repetition of the measurements in two quite different scattering geometries. The relatively large intensity of these superlattice peaks allowed such a detailed mapping of the low temperature behavior to be carried out in a reasonable amount of time.

This measured resolution function was then convoluted with the assumed cross section numerically to generate the intensity at the relevant h, k, and l coordinates for the critical scattering measurements. To yield consistent results, the data were simultaneously fit to the set of three scans along the three principal reciprocal space directions at each temperature.

A. Possible line shapes

The fluctuation-dissipation theorem relates the spin-pair correlation function, and thus the scattering cross section, to the static susceptibility.[23] The Ornstein-Zernike form for the $\mathbf{Q}$-dependent susceptibility is a Lorentzian in $\mathbf{Q}$,

$$\frac{d\sigma}{d\Omega} \sim T\chi(\mathbf{Q},T) \sim \frac{T\chi(T)}{1+\mathbf{Q}^2/\kappa^2}. \tag{4}$$

$\mathbf{Q}^2$ represents the square of the distance in reciprocal space relative to the superlattice peak position and the width κ was allowed to vary independently along h, k, and l. The full form for $\mathbf{Q}^2/\kappa^2$ for a triclinic single crystal, as was employed in the analysis, is given in the Appendix.

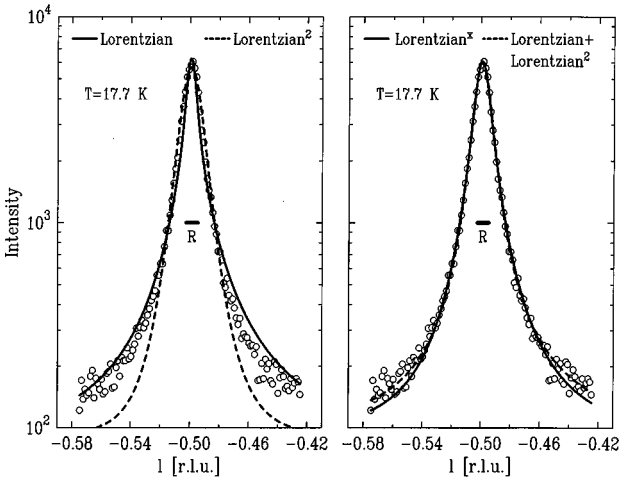

FIG. 6. The data obtained from scans along l for a temperature of about 17.7 K chosen to be clearly above the transition temperature. The solid line in the left panel indicates the best fit to a convoluted Lorentzian cross section while the dashed line represents the best fit using a Lorentzian^2 cross section. Neither are good descriptors of the data. The lines in the right panel are taken from best fits to a convoluted Lorentzian^x where x is a varying parameter (solid line) and a Lorentzian+Lorentzian^2 (dashed line). Both forms provide good descriptions of the data. For reference, the measured resolution is indicated by the horizontal bar.

Fits were performed using the convoluted Lorentzian line shape and the resulting best fit at a temperature of 17.7 K, well above the transition temperature of 17.1 K, is represented by the solid line shown in the left panel of Fig. 6. This figure shows the data taken along the l reciprocal space direction as this direction exhibited the sharpest resolution and, hence, allows for easier comparison of the fit quality (similar scans were obtained along the h and k directions). The fit to the single Lorentzian is clearly not a satisfactory description of the data as the solid line sits inside the data near the peak and overestimates the data away from the peak position. The obtained value of the goodness-of-fit parameter χ^2 at 17.7 K was 9.13 for the combined fit over the three sets of data incorporating scans along h, k, and l.

As the single Lorentzian cross section did not adequately describe the observed data, an alternative form was required. Many recent measurements of critical fluctuations using x-ray scattering have been shown to exhibit two length scales.[15] The first, describing the fluctuations in the bulk of the crystal, are well described by an Ornstein-Zernike, Lorentzian cross section with extracted critical exponents consistent with conventional universality classes. The second, larger length scale, typically well described by a Lorentzian-squared line shape, has been attributed to defects in the near-surface region and most commonly generates critical exponents larger than those obtained from the bulk fluctuations. Such observations were first made for the cubic to tetragonal structural phase transition in some of the perovskites[24–31] and later observations were made in magnetic x-ray scattering experiments on Ho-,[32,33] Tb-,[34,35] and some U-based compounds.[36–38]

The data obtained for MEM(TCNQ)$_2$ did not clearly exhibit two distinct line shapes and, consequently, fits were first attempted to a convoluted Lorentzian-squared line shape alone,

$$\frac{d\sigma}{d\Omega} \sim \frac{T\chi(T)}{(1+\mathbf{Q}^2/\kappa^2)^2}. \tag{5}$$

Such a line shape has been observed in several high-resolution synchrotron measurements including the inorganic SP system $CuGeO_3$.[14]

The best fit using the above cross section at a temperature of 17.7 K is indicated by the dashed line in the left panel of Fig. 6. One can see that this curve also does not yield an adequate description of the data, severely underestimating the data away from the peak position. The goodness-of-fit parameter for the fits at 17.7 K was 8.93, indicating a fit of equally poor quality as that provided by the single Lorentzian cross section.

As the line shape generated using Lorentzian and Lorentzian-squared cross sections produced poor descriptions of the data and there are not two distinct line shapes present in the raw data, fits were also performed using a cross section given by a Lorentzian with a varying power,

$$\frac{d\sigma}{d\Omega} \sim \frac{T\chi(T)}{(1+\mathbf{Q}^2/\kappa^2)^x}, \tag{6}$$

where x is a varying parameter of the fits. The Lorentzian cross section overestimated the scattering away from the peak position and the Lorentzian squared underestimated this same scattering; thus one would expect to obtain a best estimate of the power x lying somewhere between 1 and 2.

The best fit to such a form at a temperature of 17.7 K is represented, for the scan along the l direction, by the solid line in the right panel of Fig. 6. At this particular temperature, the best fit value of the power x was found to be 1.31, confirming the expectation of a value lying between 1 and 2. This solid line can be seen to be a much improved description of the data yielding a goodness-of-fit parameter of 1.67 at 17.7 K, a substantial improvement over the previous values for the Lorentzian or Lorentzian-squared cross sections.

To examine the progression of the obtained power x as the temperature is raised above the transition temperature, the extracted value of x, as a function of temperature, is shown in Fig. 7 for both the $(1,6,-1/2)$ and $(0,11,3/2)$ reflections. For both reflections, the value of x can be seen to decrease steadily from about 1.35 near the transition to a value of about 1, consistent with a single Lorentzian, at higher temperatures near 19 K. This indicates behavior closer to a Lorentzian squared near the transition with the data adequately described by a single Lorentzian well above T_{sp}. This observation is consistent with that observed in other systems which exhibit two-length-scale scattering. In such systems, the amplitude of the Lorentzian-squared component diminishes more rapidly with increasing temperature when compared to the corresponding Lorentzian amplitude and, eventually, the sharper fluctuations become negligible in comparison to the bulk fluctuations.

Consequently, fits were performed using a Lorentzian+Lorentzian^2 cross section,

$$\frac{d\sigma}{d\Omega} \sim \frac{T\chi_1(T)}{1+\mathbf{Q}^2/\kappa_1^2} + \frac{T\chi_2(T)}{(1+\mathbf{Q}^2/\kappa_2^2)^2}, \tag{7}$$

where the subscript 1 refers to the Lorentzian component and the subscript 2 refers to the Lorentzian squared. The best

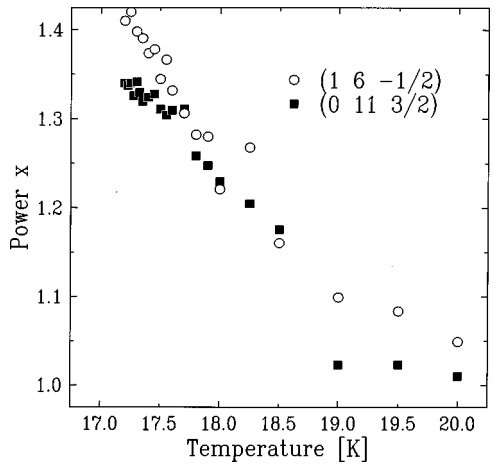

FIG. 7. The extracted power x from fits to a Lorentzian^x convoluted with the instrumental resolution as a function of temperature for both the (1,6,−1/2) and (0,11,3/2) superlattice reflections. The power of x has a best fit value of about 1.35 near T_{sp} (17.1 K) and falls off steadily with increasing temperature to a value of about unity, consistent with a single Lorentzian cross section.

description of the data using the above form is indicated by the dashed line in the right panel of Fig. 6. As was the case for the Lorentzian with a varying power, this form also describes the data very well with a resultant goodness-of-fit parameter of 1.86 at a temperature of 17.7 K. The cross sections represented by Eqs. (6) and (7) both generate excellent descriptions of the data and it is very difficult to distinguish between the two.

The discussion to this point centered on the data at a single temperature of 17.7 K chosen to be clearly above the transition temperature. To examine the behavior at differing temperatures, Table I shows the goodness-of-fit parameter χ^2 for the four cross sections discussed previously at several temperatures between 17.4 K and 20 K. The inferior nature of the fits using the Lorentzian or Lorentzian-squared cross sections in the vicinity of T_{sp} is clearly indicated by the large magnitude of χ^2. In fact, the Lorentzian^2 line shape does not appear to adequately describe the data at any temperature while the Lorentzian can be seen to produce good fit quality

TABLE I. The goodness-of-fit parameter $\chi^2=\chi_h^2+\chi_k^2+\chi_l^2$ where χ_x^2 is taken from the scan along the x direction (where $x=h$, k, or l) and $\chi_x^2=(n_i-n_{param})^{-1}\Sigma_i\{[I_{obs}(i)-I_{calc}(i)]/\Delta(I_{obs}(i))\}^2$ at several temperatures above the transition temperature. Results are shown for fits using a Lorentzian, Lorentzian^2, Lorentzian^x, Lorentzian+Lorentzian^2, and Lorentzian$^{1.35}$ cross section convoluted with the instrumental resolution function. The values shown are for the (1,6,−1/2) superlattice reflection.

T (K)	χ^2 Lor.	χ^2 Lor.^{2}	χ^2 Lor.^{x}	χ^2 Lor.+Lor.^{2}	χ^2 Lor.$^{1.35}$
17.4	29.44	15.86	2.45	3.12	2.58
17.5	23.84	14.87	2.14	2.18	2.14
17.7	9.13	8.93	1.67	1.86	1.69
18	3.87	5.99	1.87	1.77	2.12
19	1.55	3.37	1.45	2.08	1.77
20	1.50	2.53	1.50	1.66	1.71

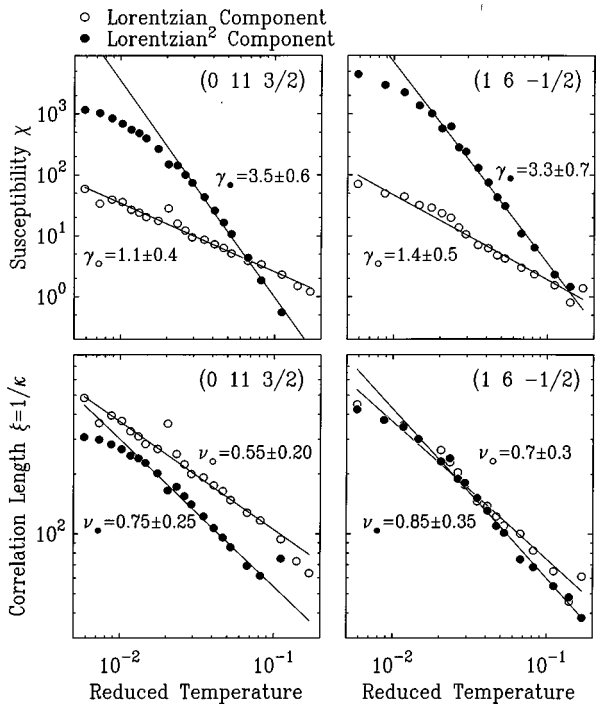

FIG. 8. The resulting susceptibility χ and the correlation length $\xi=1/\kappa$ from the fits to the Lorentzian+Lorentzian^2 cross sections convoluted with the instrumental resolution as a function of reduced temperature on a logarithmic plot for both measured superlattice reflections. The solid lines represent best fits to a power law and the resulting critical exponents are indicated on the plot where the subscript ● refers to the Lorentzian^2 component while the subscript ○ refers to the Lorentzian.

only for data sufficiently above the transition temperature. The Lorentzian with a varying power and the Lorentzian+Lorentzian^2 both generate good descriptions of the data at all temperatures and, in addition, although not previously mentioned, one can also obtain reasonable quality by fixing the varying power x to a value of about 1.35. This value corresponds to that obtained for temperatures close to the transition temperature and the resulting goodness-of-fit parameters using such a cross section are shown in the last column of Table I. Thus, we have shown that the Lorentzian cross section expected for Ornstein-Zernike fluctuations does not adequately describe the data near T_{sp} and have provided three alternative forms which produce good descriptions of the data.

B. Critical exponents

Of the possible cross sections which produce reasonable descriptions of the data, the only one expected to yield meaningful exponents is the Lorentzian+Lorentzian^2, Eq. (7). This expectation is derived from previous x-ray and neutron measurements of critical scattering where two length scales were observed.[15] The resulting susceptibility χ_1 and the correlation length $\xi_1\sim 1/\kappa_1$ versus reduced temperature, with $T_{sp}=17.1$ K, is shown in Fig. 8 on a logarithmic plot. Initially, the width κ_1 was allowed to vary independently along h, k, and l, but the widths were found to be related to each other by a simple multiplicative constant and, hence, the values along k and l were fixed to be some ratio of the width along h to lower the number of varying fit parameters. The

widths for the Lorentzian and Lorentzian^2 components were allowed to vary independently. Scaling theory of continuous phase transitions indicates that both χ_1 and ξ_1 should obey power law behavior in the immediate vicinity of T_{sp},

$$\chi_1 \sim t^{-\gamma_1}, \quad \xi_1 \sim t^{-\nu_1}, \tag{8}$$

where the critical exponents γ_1 and ν_1 are universal quantities which help to define the universality class for a given phase transition.

The solid lines shown in Fig. 8 represent the best power law description of the data and yield exponents for the Lorentzian component of the line shape of $\gamma_1 = 1.1 \pm 0.4$ and $\gamma_1 = 1.4 \pm 0.5$ for the (0,11,3/2) and (1,6,$-1/2$) reflections with corresponding values of ν_1 of 0.55 ± 0.20 and 0.7 ± 0.3. Such values are indeed consistent with conventional 3D behavior as suggested from the detailed order parameter analysis presented previously [the theoretical values of γ for 3D Ising, XY, and Heisenberg behavior are 1.24, 1.32, and 1.39, respectively, with corresponding values of ν of 0.63, 0.67, and 0.71 (Ref. 20)]. The relatively large error bars on these critical exponent determinations do not allow distinction between 3D behavior and mean field behavior [where $\gamma = 1$ and $\nu = 0.5$ (Ref. 39)] as was possible with the exponent β extracted from the order parameter. However, all previous measurements of two-length-scale scattering have occurred in systems exhibiting non-mean-field critical behavior.[15] This may suggest that the potential observation of such scattering in MEM(TCNQ)$_2$ is, in itself, indicative of critical behavior inconsistent with mean field theory, as confirmed by the β exponent determination.

Although the extracted exponents are largely meaningless in terms of the assignment of a universality class, fits to the power law represented by Eq. (8) were also performed for the Lorentzian^2 component. The exponents obtained can be seen to be consistent between the two superlattice reflections yielding values of γ_2 of 3.5 ± 0.6 and 3.3 ± 0.7 and values of ν_2 of 0.75 ± 0.25 and 0.85 ± 0.35 for the (0,11,3/2) and (1,6,$-1/2$) reflections, respectively. As had been suggested from previous second-length-scale observations,[15] these exponents are larger than those obtained for the bulk exponents, particularly for the exponent γ describing the susceptibility. One can also see from the data presented in Fig. 8 that the Lorentzian^2 component only seems to exhibit power law behavior for reduced temperatures in excess of about 0.02, deviating substantially from the solid line below this value. The nature of such a deviation is unclear and may be indicative of either problems with the Lorentzian+Lorentzian^2 description of the data for temperatures very close to T_{sp} or a crossover to a regime where the two components exhibit similar exponents.

C. Discussion

The observed scattering appears to produce results consistent with the observation of two length scales in previous x-ray scattering measurements but there are a number of striking differences which should be mentioned. The most significant difference is the relative magnitude of the correlation lengths for the Lorentzian and Lorentzian^2 components. The best fit width κ for the Lorentzian component of the line shape is the same size or smaller than the corresponding width for the Lorentzian^2 component as can be seen from the extracted widths in the lower panel of Fig. 8 and also from Fig. 9 where the Lorentzian+Lorentzian^2 components of the best fit at 17.7 K are shown. This indicates a length scale for the Lorentzian component which is of roughly the same size or perhaps even larger than the associated length scale for the Lorentzian^2 portion. This is in contrast to the majority of two-length-scale observations obtained previously where the Lorentzian^2 is noticeably sharper in **Q** indicating a larger associated length scale.[15]

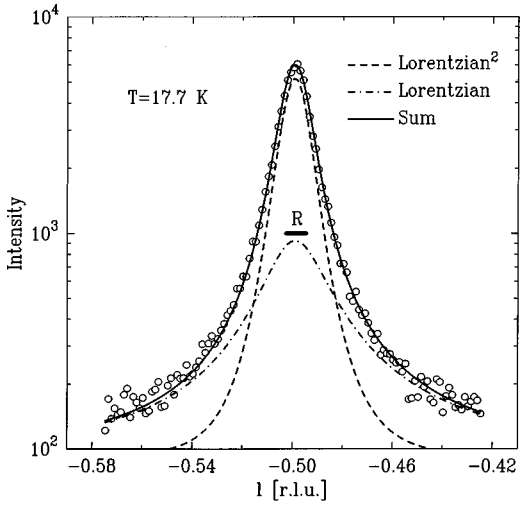

FIG. 9. The data obtained for a scan along l at a temperature of 17.7 K. The solid line shows the best fit to a Lorentzian+Lorentzian^2 cross section convoluted with the instrumental resolution. The dashed line shows the Lorentzian^2 component of this best fit and the dash-dotted line shows the Lorentzian component. For reference, the resolution is indicated by the horizontal bar.

The second difference between these observations and typical two-length-scale measurements is in the falloff of the Lorentzian^2 component. Most measurements show the presence of a sharp Lorentzian^2 line shape which usually disappears with increasing temperature by a reduced temperature of about 0.04.[15] From Fig. 8, one can clearly see that the Lorentzian^2 remains until a reduced temperature of about 0.1 above which the observed scattering is well described by a single Lorentzian.

The appearance of two-length-scale scattering is typically observed in the presence of substantial surface sensitivity, as is the case for most x-ray scattering measurements resulting from relatively small penetration depths. This fact is partially responsible for the characterization of the second length scale as a near-surface effect. However, the organic nature of MEM(TCNQ)$_2$ should produce large penetration depths for the 8-keV x rays employed in this study and, consequently, surface sensitivity is weak. As a result, this measurement more closely resembles typical neutron scattering experiments where large penetration depths cause the bulk of the crystal to be sampled and, in such measurements, only one length scale is typically observed. The potential observation of such scattering in MEM(TCNQ)$_2$ is unexpected. It is possible that it may have resulted from a sampled scattering

volume which overlapped with a large section of the near-surface region, yielding substantial surface sensitivity despite the large penetration depths. Such a possibility is more likely with x rays than with neutrons as distance collimation employed in x-ray measurements results in a very narrow beam and a resulting small scattering volume, whereas with neutrons, collimation is typically provided by Soller slits producing a beam with a size on the order of a few centimeters. The observation of such scattering at two distinct wave vectors seems inconsistent with such a possibility as the scattering geometries differ greatly between the two. However, the ratio of amplitudes for the Lorentzian to Lorentzian^2 components differs between the two reflections by a factor of 3. This indicates a much weaker Lorentzian^2 component at the (0,11,3/2) reflection, a difference which could be attributed to differences in scattering geometry.

A similar scenario has been observed previously with high-energy synchrotron x-ray experiments performed on the perovskite $SrTiO_3$.[27] In these experiments, high-energy ($\sim$100 keV) x rays were used in an attempt to increase the penetration depths. As a result, only a single-component line shape, well described by a Lorentzian, was observed with a temperature dependence consistent with neutron measurements. However, when the experiment was configured to sample a near-surface volume element, the second length scale was observed.

Another possible explanation of the existence of a two-component line shape is that such a cross section is intrinsic to the system and not a consequence of defects in the near surface region. The observation of such scattering in $MEM(TCNQ)_2$ with no obvious surface sensitivity would seem to be consistent with such a possibility. This possibility was discussed by Cowley,[15] and if such an explanation is correct, it indicates shortcomings in the scaling theory of continuous phase transitions when applied to such a system using such a probe.

Although we cannot distinguish between the three possible line shapes, the observed scattering bears a striking resemblance to previous neutron measurements on a dilute 2D random Ising antiferromagnet in a magnetic field.[40] In these measurements, scattering was observed which was not well described by a single Lorentzian line shape and the suggested line shapes were identical to those reported in this paper, namely, a Lorentzian with a varying power and a Lorentzian+Lorentzian^2. Indeed it was such similarities which led to the possible description of the two-length-scale scattering in terms of random defects distributed in the quasi-two-dimensional near-surface region.

VI. SUMMARY

Measurements of the temperature dependence of the intensity of the superlattice Bragg peaks indicate a transition temperature of 17.1 ± 0.2 K and an order parameter characterized by a critical exponent β of 0.35 ± 0.06. This exponent is consistent with conventional 3D universality as observed previously in the inorganic SP compound $CuGeO_3$ and is clearly inconsistent with previous measurements where behavior consistent with mean field theory was reported. Analysis of the critical behavior of the order parameter indicated that the correction-to-scaling term is not needed for temperatures as low as 2 K below the transition temperature. This indicates a much gentler variation of the order parameter as compared with $CuGeO_3$ where the correction term was needed for temperatures within about 0.5 K of the transition temperature.

Lattice constant measurements on the (0,0,4) and (0,12,0) Bragg reflections indicate the presence of spontaneous strains below the transition temperature as observed in previous work on $CuGeO_3$. The observation of such spontaneous strains in an organic SP system suggests that their presence is an intrinsic characteristic of the SP phase transition.

Measurements of fluctuations indicate the presence of substantial critical scattering, as had been observed previously. This scattering, however, cannot be adequately described by a single Lorentzian line shape as expected from the scaling theory of continuous phase transitions. The data can be adequately described by a Lorentzian with a varying power or a Lorentzian+Lorentzian^2. Similar line shapes have previously been observed in x-ray scattering measurements of critical fluctuations where two length scales are observed, one corresponding to the bulk fluctuations well described by a Lorentzian while the second, larger length scale is typically well described by a Lorentzian^2. Analysis using this form for the cross section allows bulk exponents γ and ν to be extracted from the Lorentzian component and such an effort yields exponents consistent with 3D behavior, as seen with the order parameter, but not inconsistent with mean field theory. Exponents extracted from the Lorentzian^2 portion of the line shape are larger than those for the Lorentzian component, particularly for γ, in a manner similar to previous two-length-scale studies.

ACKNOWLEDGMENTS

This work was supported by NSERC of Canada and OCMR of Ontario. We thank H.A. Mook for making the single crystal available to us.

APPENDIX: FULL FORM OF Q^2 FOR A TRICLINIC CRYSTAL

The square of the distance in reciprocal space Q^2 for a triclinic single crystal with lattice parameters $a, b, c, \alpha, \beta, \gamma$ in terms of the Miller indices h, k, l, can be shown to be

$$\begin{aligned} Q^2 = 4\pi^2 & (1+2\cos\alpha\cos\beta\cos\gamma \\ & -\cos^2\alpha-\cos^2\beta-\cos^2\gamma)^{-1} \\ & \times\left[\sin^2\alpha\frac{h^2}{a^2}+\sin^2\beta\frac{k^2}{b^2}+\sin^2\gamma\frac{l^2}{c^2}\right. \\ & +2(\cos\alpha\cos\beta-\cos\gamma)\frac{hk}{ab}+2(\cos\beta\cos\gamma \\ & \left.-\cos\alpha)\frac{kl}{bc}+2(\cos\gamma\cos\alpha-\cos\beta)\frac{hl}{ac}\right]. \end{aligned} \quad \text{(A1)}$$

The distance in reciprocal space away from some position, h',k',l', divided by a width κ with allowance for differing widths along h, k, l will then be given by

$$\frac{Q^2}{\kappa^2} = 4\pi^2(1+2\cos\alpha\cos\beta\cos\gamma-\cos^2\alpha-\cos^2\beta-\cos^2\gamma)^{-1}\times\left[\frac{\sin^2\alpha}{a^2}\frac{(h-h')^2}{\kappa_h^2}+\frac{\sin^2\beta}{b^2}\frac{(k-k')^2}{\kappa_k^2}+\frac{\sin^2\gamma}{c^2}\frac{(l-l')^2}{\kappa_l^2}+2\frac{(\cos\alpha\cos\beta-\cos\gamma)}{ab}\frac{(h-h')(k-k')}{\kappa_h\kappa_k}+2\frac{(\cos\beta\cos\gamma-\cos\alpha)}{bc}\frac{(k-k')(l-l')}{\kappa_k\kappa_l}+2\frac{(\cos\gamma\cos\alpha-\cos\beta)}{ac}\frac{(h-h')(l-l')}{\kappa_h\kappa_l}\right]. \quad \text{(A2)}$$

The above equation is the full expression which is substituted for Q^2/κ^2 in Eqs. (4), (5), (6), and (7).

[1] See J. W. Bray, L. V. Interrante, I. S. Jacobs, and J. C. Bonner, in *Extended Linear Chain Compounds*, edited by J. S. Miller (Plenum Press, New York, 1983), Vol. 3, p. 353, and references therein.

[2] B. van Bodegom, Acta Crystallogr., Sect. B: Struct. Crystallogr. Cryst. Chem. **37**, 863 (1981).

[3] S. Huizinga, J. Kommandeur, G. A. Sawatzky, B. T. Thole, K. Kopinga, W. J. M. de Jonge, and J. Roos, Phys. Rev. B **19**, 4723 (1979).

[4] B. van Bodegom, B. C. Larson, and H. A. Mook, Phys. Rev. B **24**, 1520 (1981).

[5] P. I. Kuindersma, G. A. Sawatzky, and J. Kommandeur, J. Phys. C **8**, 3005 (1975).

[6] R. J. J. Visser, S. Oostra, C. Vettier, and J. Voiron, Phys. Rev. B **28**, 2074 (1983).

[7] G. Aeppli, J. L. deBoer, J. P. Pouget, and G. Shirane, Phys. Rev. B **29**, 5165 (1984).

[8] S. J. Blundell, F. L. Pratt, P. A. Pattenden, M. Kurmoo, K. H. Chow, S. Tagagi, Zh. Jestädt, and W. Hayes, J. Phys.: Condens. Matter **9**, L119 (1997).

[9] D. Bloch, J. Voiron, J. W. Bray, I. S. Jacobs, J. C. Bonner, and J. Kommandeur, Phys. Lett. **82A**, 21 (1981).

[10] M. D. Lumsden, B. D. Gaulin, and H. Dabkowska, Phys. Rev. B **57**, 14 097 (1998).

[11] J. P. Pouget, L. P. Regnault, M. Ain, B. Hennion, J. P. Renard, P. Veillet, G. Dhalenne, and A. Revocolevschi, Phys. Rev. Lett. **72**, 4037 (1994).

[12] K. Hirota, D. E. Cox, J. E. Lorenzo, G. Shirane, J. M. Tranquada, M. Hase, K. Uchinokura, H. Kojima, Y. Shibuya, and I. Tanaka, Phys. Rev. Lett. **73**, 736 (1994).

[13] Q. J. Harris, Q. Feng, R. J. Birgeneau, K. Hirota, K. Kakurai, J. E. Lorenzo, G. Shirane, M. Hase, K. Uchinokura, H. Kojima, I. Tanaka, and Y. Shibuya, Phys. Rev. B **50**, 12 606 (1994).

[14] Q. J. Harris, Q. Feng, R. J. Birgeneau, K. Hirota, G. Shirane, M. Hase, and K. Uchinokura, Phys. Rev. B **52**, 15 420 (1995).

[15] A good review of two-length-scale phenomena is provided in R. A. Cowley, Phys. Scr. **T66**, 24 (1996).

[16] D. E. Moncton, R. J. Birgeneau, L. V. Interrante, and F. Wudl, Phys. Rev. Lett. **39**, 507 (1977).

[17] J. E. Lorenzo, K. Hirota, G. Shirane, J. M. Tranquada, M. Hase, K. Uchinokura, H. Kojima, I. Tanaka, and Y. Shibuya, Phys. Rev. B **50**, 1278 (1994).

[18] H. Winkelmann, E. Gamper, B. Büchner, M. Braden, A. Revcolevschi, and G. Dhalenne, Phys. Rev. B **51**, 12 884 (1995).

[19] A. Aharony and G. Ahlers, Phys. Rev. Lett. **44**, 782 (1980).

[20] M. F. Collins, *Magnetic Critical Scattering* (Oxford University Press, New York, 1989).

[21] Y. Tanaka, N. Satoh, and K. Nagasaka, J. Phys. Soc. Jpn. **59**, 319 (1990).

[22] M. Köppen, D. Pankert, R. Hauptmann, M. Lang, M. Weiden, C. Geibel, and F. Steglich, Phys. Rev. B **57**, 8466 (1998).

[23] H. Eugene Stanley, *Introduction to Phase Transitions and Critical Phenomena* (Clarendon Press, Oxford, 1971).

[24] S. R. Andrews, J. Phys. C **19**, 3721 (1986).

[25] R. J. Nelmes, P. E. Hatton, and H. Vass, Phys. Rev. Lett. **60**, 2172 (1988).

[26] D. F. McMorrow, N. Hamaya, S. Shimomura, Y. Fujii, S. Kishimoto, and H. Iwasaki, Solid State Commun. **76**, 443 (1990).

[27] H.-B. Neumann, U. Rütt, J. R. Schneider, and G. Shirane, Phys. Rev. B **52**, 3981 (1995).

[28] K. Hirota, J. P. Hill, S. M. Shapiro, G. Shirane, and Y. Fujii, Phys. Rev. B **52**, 13 195 (1995).

[29] U. J. Nicholls and R. A. Cowley, J. Phys. C **20**, 3417 (1987).

[30] T. W. Ryan, R. J. Nelmes, R. A. Cowley, and A. Gibaud, Phys. Rev. Lett. **56**, 2704 (1986).

[31] A. Gibaud, R. A. Cowley, and P. W. Mitchell, J. Phys. C **20**, 3849 (1987).

[32] T. R. Thurston, G. Helgesen, Doon Gibbs, J. P. Hill, B. D. Gaulin, and G. Shirane, Phys. Rev. Lett. **70**, 3151 (1993).

[33] T. R. Thurston, G. Helgesen, J. P. Hill, Doon Gibbs, B. D. Gaulin, and P. J. Simpson, Phys. Rev. B **49**, 15 730 (1994).

[34] K. Hirota, G. Shirane, P. M. Gehring, and C. F. Majkrzak, Phys. Rev. B **49**, 11 967 (1994).

[35] P. M. Gehring, K. Hirota, C. F. Majkrzak, and G. Shirane, Phys. Rev. B **51**, 3234 (1995).

[36] G. M. Watson, B. D. Gaulin, Doon Gibbs, T. R. Thurston, P. J. Simpson, S. M. Shapiro, G. H. Lander, Hj. Matzke, S. Wang, and M. Dudley, Phys. Rev. B **53**, 686 (1996).

[37] S. G. Perry, W. J. Nuttall, W. G. Stirling, G. H. Lander, and O. Vogt, Phys. Rev. B **54**, 15 234 (1996).

[38] A. Stunault, S. Langridge, C. Vettier, Doon Gibbs, and N. Bernhoeft, Phys. Rev. B **55**, 423 (1997).

[39] See, for example, M. Plischke and B. Bergersen, *Equilibrium Statistical Physics* (Prentice Hall, Englewood Cliffs, NJ, 1989).

[40] R. J. Birgeneau, H. Yoshizawa, R. A. Cowley, G. Shirane, and H. Ikeda, Phys. Rev. B **28**, 1438 (1983).